Modified spontaneous emission from laterally injected photonic crystal emitter

C.M. Long, A.V. Giannopoulos and K.D. Choquette

The first use of lateral current injection to excite membrane photonic crystal light emitters is reported. The devices utilise a transverse diode that is created via ion implantation into a 280 nm-thick InGaAsP membrane. Photonic bandgap effects and spectral tuning of the electroluminescence spectra due to the graphene geometry photonic crystal are presented.

Introduction: Photonic crystals (PhC) have created new possibilities within photonics to control light emission. Through careful design, the dispersive properties of a material can be engineered via PhCs, which has been exploited to create ultra-small lasers [1, 2], high-Q cavities [3], and band edge photonic crystal lasers [4]. The devices are usually pumped through optical excitation, with only a few exceptions [5–7]. Direct electrical excitation will be more practical, but this is a difficult, delicate task owing to the often-conflicting requirements necessary to obtain good electrical, thermal and optical properties within the device. A novel design and fabrication method is necessary to simultaneously meet these demands. In this Letter, the lateral current injection (LCI) PhC emitter is introduced, whereby a transverse diode is created within a semiconductor membrane with ion implantation and a PhC is patterned at the diode junction.

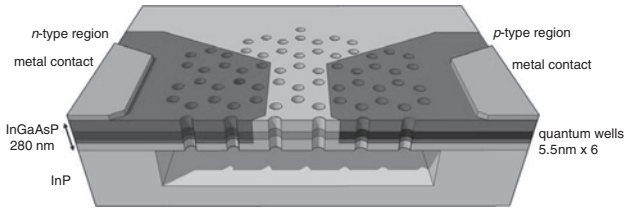

Fig. 1 *Schematic of LCI PhC emitter, shown in cross-section*

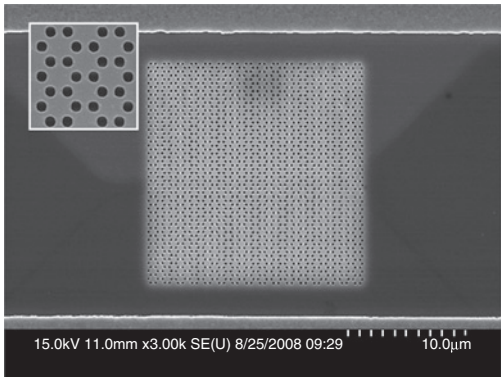

Fig. 2 *SEM image of LCI graphene PhC with metal contacts; also visible are doped regions of diode*

Inset: magnified view of graphene lattice

Fabrication and design: A schematic of the completed LCI PhC is shown in Fig. 1. The devices are fabricated in a membrane of InGaAsP, unintentionally doped, and epitaxially grown on an InP substrate. The membrane has a thickness of 280 nm and contains six strain-compensated quantum wells with peak emission at 1550 nm. Metal alignment marks are deposited, followed by a layer of SiN to serve as an implantation mask. Si is implanted to dope the n-type regions to a concentration of $5 \times 10^{18}/\text{cm}^3$. The SiN masking layer is removed and the SiN mask layer process is repeated, followed by Be implantation to create the p-type regions. After removal of all SiN, the sample is heated to 800°C for 5 s to anneal the implantation damage and activate the dopants. Two separate metal layers are deposited in order to make contact to the n- and p-regions, and then sintered at 400°C for 30 s. Next, a layer of SiO_2 is deposited onto the sample via plasma enhanced chemical vapour deposition (PECVD). A layer of polymethylmethacrylate (PMMA) e-beam resist is spun on and patterned using electron-beam lithography. The patterns are transferred into the SiO_2 using Freon-23 plasma and then etched into the semiconductor using an inductively coupled plasma reactive ion etcher. The last step is to selectively remove the underlying InP with a room temperature wet etch. An SEM image of a completed LCI PhC emitter is shown in Fig. 2. The metal contacts are visible along the horizontal edges of the image, and the doped regions have different contrast from the undoped semiconductor; the p–n junction lies in the middle of the PhC.

The type of PhC employed is a key factor in creating an electrically-injected device because of the adaptations necessary to reduce electrical resistance and carrier loss. In this work, we employ bulk PhCs possessing a graphene structure [8]. This structure is based on a regular hexagonal lattice but with a periodic defect placed every $\sqrt{3}$ times the lattice constant (see inset of Fig. 2). Its main advantage over hexagonal lattices is that it increases the amount of semiconductor material within a unit cell. This will increase the average cross-sectional area of the current path and reduces the amount of loss introduced by non-radiative sidewall recombination of the carriers. Benefits are also seen in the electromagnetic modes propagating within the device. The graphene structure supports electromagnetic modes that have greater spatial overlap between the electromagnetic field and the gain regions when compared to a hexagonal lattice, thus improving coupling between the gain and the field.

Characterisation: After fabrication, transverse diodes without PhCs show a forward differential resistance of 600 Ω and a reverse breakdown voltage of >20 V. Patterning and etching the graphene PhC causes the resistance to increase only slightly. Since no additional steps are taken to separate the anode and cathode of the transverse p–n junction outside of the PhC pattern, a considerable amount of current is shunted around the highly-resistive PhC rather than flowing through it.

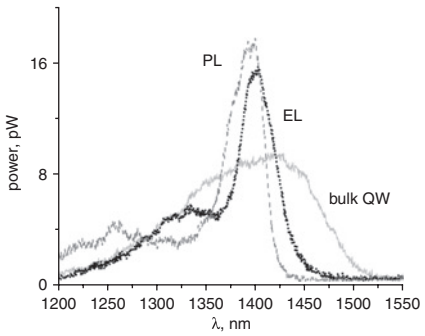

Fig. 3 *Emission spectra of LCI PhC: EL from an unpatterned quantum well, EL from the PhC, and PL from the PhC*

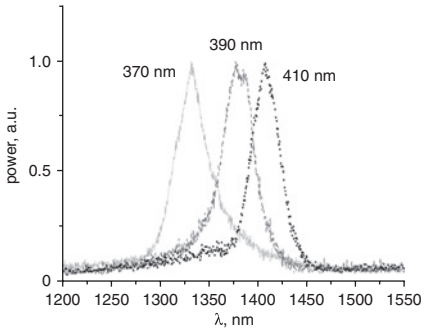

Fig. 4 *Resonance tuning of EL spectra from graphene PhCs with differing lattice constants*

The emission spectra are collected using a lensed singlemode fibre probe that is positioned directly above the device under test. Fig. 3 shows the electroluminescence (EL) spectrum from a region of unpatterned and unetched quantum well, the EL spectrum of a bulk graphene PhC, and a photoluminescence (PL) spectrum for the device. The EL spectra are obtained by positioning the fibre in two different locations along the diode junction and separated by a few microns. The device is biased with 13 V pulses that are 100 ns in width and have 30% duty cycle. The EL and PL spectra clearly show the bandgap effect of the PhC; spontaneous emission is suppressed for wavelengths longer than 1450 nm as compared to the bulk EL, and increased at the band edge of approximately 1420 nm. The slight differences between the

PL and EL spectra can be attributed to differences in size of the collection area and pumping levels. Multiple graphene PhC patterns were created with a radius-to-nearest-neighbour-spacing ratio of 0.31 for spacings in the range 370–410 nm. As shown in Fig. 4, the spectral resonance arising from the band edge decreases to a shorter wavelength as the lattice constant decreases, as expected, further illustrating the PhC control of the spontaneous emission modes.

Conclusions: A novel membrane diode emitter is introduced that incorporates a PhC into a transverse diode junction. The gain within the semiconductor quantum wells interacts with the PhC, inhibiting light emission at some wavelengths and enhancing it at others. One application for this new device topology would be active photonic integrated circuits. In a photonic circuit, the individual circuit elements require independent control, so it is necessary to add gain selectively into different regions. In addition, the active devices can be linked using passive (non-lossy) waveguides. The LCI approach can provide the flexibility and robustness necessary to create electrically-injected light sources in a photonic circuit.

Acknowledgment: This work was partially supported by DARPA under award no. 433143874.

26 September 2008
Electronics Letters online no: 20092784
doi: 10.1049/el:20092784

C.M. Long, A.V. Giannopoulos and K.D. Choquette (*Department of Electrical and Computer Engineering, University of Illinois, 208 N. Wright Street, Urbana, IL 61801, USA*)

E-mail: choquett@illinois.edu

References

1 Painter, O., Lee, R.K., Sherer, A., Yariv, A., O'Brien, J.D., Dapkus, P.D., and Kim, I.: 'Two-dimensional photonic band-gap defect mode laser', *Science*, 1999, **284**, pp. 1819–1821
2 Park, H.G., Hwang, J.K., Huh, J., Ryu, H.Y., Kim, S.H., Kim, J.S., and Lee, Y.H.: 'Characteristics of modified single-defect two-dimensional photonic crystal lasers', *IEEE J. Quantum Electron.*, 2002, **38**, pp. 1353–1365
3 Song, B.S., Noda, S., Asano, T., and Akahane, Y.: 'Ultra-high-Q photonic double-heterostructure nanocavity', *Nature Mater.*, 2005, **4**, pp. 207–210
4 Ryu, H.Y., Kwon, S.H., Lee, Y.J., Lee, Y.H., and Kim, J.S.: 'Very-low-threshold photonic band-edge lasers from free-standing triangular photonic crystal slabs', *Appl. Phys. Lett.*, 2002, **80**, pp. 3476–3478
5 Imada, M., Noda, S., Chutinan, A., Tokuda, T., Murata, M., and Sasaki, G.: 'Coherent two-dimensional lasing action in surface-emitting laser with triangular-lattice photonic crystal structure', *Appl. Phys. Lett.*, 1999, **75**, pp. 316–318
6 Park, H.G., Kim, S.H., Seo, M.K., Ju, Y.G., Kim, S.B., and Lee, Y.H.: 'Characteristics of electrically driven two-dimensional photonic crystal lasers', *IEEE J. Quantum Electron.*, 2005, **41**, pp. 1131–1141
7 Chakravarty, S., Battacharya, P., and Mi, Z.: 'Electrically injected quantum-dot photonic crystal microcavity light-emitting arrays with air-bridge contacts', *IEEE Photonics Technol. Lett.*, 2006, **18**, pp. 2665–2667
8 Cassagne, D., Jouanin, C., and Bertho, D.: 'Photonic band gaps in a two-dimensional graphite structure', *Phys. Rev. B*, 1995, **52**, R2217–R2220